ORIGINAL ARTICLE

Nr 2025;15 (1):42-56

# Acute Structural Repercussions of Vertical Ladder Training on the Muscle Belly of *Wistar Rats* after Joint Immobilization

**Bruna Aléxia Cristofoletti Grillo, André Neri Tomiate, Jurandyr Pimentel Neto, José Roberto Rodrigues da Silva, Adriano Polican Ciena**

*Laboratory of Morphology and Physical Activity (LAMAF), Institute of Biosciences, São Paulo State University (UNESP), Rio Claro, SP, Brazil*
*The authors contributed equally to this work*

**CORRESPONDING AUTHOR:**
Adriano Polican Ciena
Laboratory of Morphology and Physical Activity (LAMAF)
Institute of Biosciences
São Paulo State University (UNESP)
24A Avenue, 1515
13506-900 Rio Claro-SP, Brazil
E-mail: adriano.ciena@unesp.br

**DOI:**
10.32098/mltj.01.2025.06

**LEVEL OF EVIDENCE:** N/A (Animal study)

**SUMMARY**

**Background.** Resistance training promotes positive musculoskeletal adaptations that reverse changes in long-term muscle atrophy, elucidating the progression and coordination of acute muscle remodeling caused by resistance training without additional load.

**Objective.** The aim was to describe the morphological changes and the acute period of remodeling in the gastrocnemius muscle, after muscular atrophy caused by joint immobilization and intervention with vertical ladder training in *Wistar* rats.

**Methods.** Sixty-five 60-day-old *Wistar* rats were divided into: Control (C); Trained (T); Immobilized (I); Post-immobilization (PI); Trained Immobilized (TI). The groups were analyzed in 4 periods (0-hours, 24-hours, 4-days, and 7-days), therefore, the animals had intervention levels of the protocols. By light microscopy were measured the complexity of the nuclei through fractal dimension (FD), quantification of connective tissue, and with Myofibrillar ATPase, the cross-sectional area (CSA) of type I and II fibers.

**Results.** Isolated training promoted less FD (T0h) followed by an increase (T24h), reduction of the connective tissue (T0h) with accentuated increase (T24h), and progression of CSA (TI0h, TI24h, TI4d, TI7d). Immobilization resulted in reduced FD (I0h), an increase in connective tissue (I0h), and reductions in muscle fiber CSA (I0h, PI24h). While training after atrophy promoted an increase in the FD (TI0h), variations in the connective tissue (TI0h, TI4d, TI7d), and an increase in CSA (TI0h, TI4d, TI7d).

**Conclusions.** Resistance training promoted changes in the myonuclei, connective tissue, and CSA of muscle fibers since the 1st session, which inhibits the progression of atrophic effects even after interruption of the atrophy protocol.

**KEY WORDS**

*Muscle atrophy; resistance training; immobilization; morphometry; intramuscular connective tissue.*

## INTRODUCTION

The locomotor apparatus comprises several structures that stand out for their morphofunctional and adaptive characteristics, such as striated skeletal muscle. Skeletal muscle tissue is composed of a complex and unique arrangement of cylindrical, elongated, and multinucleated cells called muscle fibers, which act in the contractile function, are also responsible for postural maintenance and energy homeostasis (1).

From a metabolic point of view, muscle fibers are distinguished into two main types: I, which have a greater blood supply, with a large density of mitochondria for the activa-

tion of oxidative pathways. While type II fibers are characterized by their high glycolytic capacity (2).

In addition to muscle fibers, skeletal striated muscle is composed of other structures that assist in the function and preponderant structure of this tissue, in addition to ensuring structural integrity and postnatal remodeling, including: intramuscular connective tissue, formed by a complex network of envelopes, composed of collagens, non-collagenous glycoproteins, proteoglycans, and elastin; nuclei, essential for homeostasis, maintenance and adaptive responses of skeletal muscle, since their transcriptional activities act on protein synthesis; and satellite cells, which remain in a quiescent state, and a disturbed situation, are activated, proliferate, differentiate and fuse, to form or repair the muscle fiber (1, 3-7).

Muscular atrophy is a condition characterized by the loss of muscle mass caused by several intrinsic and extrinsic factors, which are present worldwide and contribute to high morbidity and mortality (8-11). Regardless of the origin of muscular atrophy, this condition seriously impacts the quality of life, as it reduces the mobility and strength, and consequently, makes it difficult to carry out daily activities (12).

The loss of muscle mass that defines muscle atrophy results from the hyperactivation of protein degradation signaling pathways in muscle atrophy, including the ubiquitin-proteasome system, autophagy-lysosome system, and caspase system, and results in the net loss of myofibrillar proteins, organelles, and cytoplasm (12-14).

In the morphology of skeletal striated muscle, muscular atrophy causes changes that lead to morphofunctional impairment. Such as a reduction in protein content, thus there is a decrease in the cross-sectional area (CSA) of the fiber. In addition, there is an increase in intramuscular connective tissue, a decrease in capillary density, rupture of the three-dimensional architecture, reduced mitochondrial density, elevated intramuscular calcium levels, myonuclear apoptosis, and a decreased number of satellite cells (7,15).

Consequently, these structural adaptations in skeletal striated muscle contribute to the decline of the locomotor system, which harms quality of life by making it difficult to carry out daily activities and prolong recovery after comorbidities. Therefore, it is essential to implement interventions, such as physical training, to reduce muscular vulnerability to injuries (12).

Physical training is characterized by mechanical overload, capable of initiating regenerative processes towards positive remodeling of skeletal striated muscle (13, 16). In an experimental model, resistance training can be performed with or without additional overload to the animals' muscle mass. The main adaptations promoted include the suppression of inflammation, radial growth of muscle fibers, increase in myonuclei, and mitochondrial and vascular expansion, in addition to improvement of satellite cell proliferation (14, 17, 18).

The ability to promote a regenerative environment right after the first hours (acute period) of training intervention, since significant reductions in atrophic pathways occur due to the reduction in the levels of ubiquitin ligases 3 (19). Therefore, the positive repercussions of training are a cumulative effect of each exercise session's acute adaptations, making it an effective option for reversing harmful remodeling, especially elucidating the progression and coordination of musculoskeletal remodeling.

However, the acute and chronic changes described after the training intervention encompass different modalities expressing high load or volume. The study aimed to describe the morphological changes and the acute period of remodeling in the gastrocnemius muscle, after muscular atrophy caused by joint immobilization and intervention with vertical ladder training in *Wistar* rats.

## MATERIALS AND METHODS

### Animals

Sixty-five 60-day-old *Wistar* rats were randomly divided into 5 groups: Control (C): submitted to no protocol; Trained (T): submitted to the vertical ladder training protocol; Immobilized (I): subjected to the muscular atrophy protocol (joint immobilization); Post-immobilization (PI): subjected to the muscular atrophy protocol (joint immobilization) followed by free movement; Trained Immobilized (TI): subjected to the muscular atrophy protocol (joint immobilization) and vertical ladder training.

For the temporal analysis of the remodeling of the gastrocnemius muscle, 4 collection periods were carried out with 5 animals/group/period, thus, the animals had different ages and intervention levels of the protocols. The collection periods carried out were:

- 0-hour period (P0h): at 70 days, the muscular atrophy protocol was completed with the removal of the immobilization devices from Group I, PI, and TI, and the animals from Groups T and TI were subjected to the 1st session of vertical ladder training. According to the Group, the animals euthanized during this period formed the subgroups: C, T0h, I0h, and TI0h;
- 24-hour period (P24h): at 71 days, animals from all Groups were not subjected to any protocol, thus, animals

from Groups PI and TI were free to move for 24 hours, while Groups T and TI completed 24 hours of the 1st training session. At P24h, the animals from each Group formed the subgroups: T24h, PI24h, and TI24h;

- 4-day period (P4d): at 74 days, the animals in Groups PI and TI had been free to move for 4 days, and Groups T and TI underwent the next vertical ladder training sessions (2nd and 3rd) with days of alternate rest. At the end of the 3rd training session (4th day), samples were collected from the subgroups: T4d, PI4d and TI4d;
- 7-day period (P7d): at 77 days, 7 days after the end of the muscular atrophy protocol, the animals in Group PI completed 7 days without intervention, with only free movement, while the animals in groups T and TI performed the 4th vertical ladder training session (7th day). After the training session, samples were collected from all remaining animals, which comprised the subgroups: T7d, PI7d, and TI7d.

All animals came from the Central Animal Facility of UNESP - Botucatu - SP, and were housed in the Animal House of the Human Anatomy Laboratory - Institute of Biosciences of UNESP-Rio Claro-SP. The animals were maintained at a controlled temperature (23 ± 2 °C), light/dark photoperiod, and with food and water *ad libitum*. The procedures presented in this study were previously approved by the Ethics Committee on the Use of Animals - CEUA of the Institute of Biosciences of the São Paulo State University - Rio Claro-SP (nº 06/2022 - date of approval: September 14, 2022).

## Joint immobilization

At 60 days of age, animals from Groups I, PI, and TI were subjected to the immobilization protocol for 10 days. Joint immobilization was performed in 6 stages: 1) Intramuscular anesthesia (Ketamine 95 mg/kg and Xylazine 12 mg/kg); 2) Immobilization of the tibiotarsal joint in maximum plantar flexion of the right hind limb with the aid of the micropore; 3) Insertion of the shirt, which will be used as an upper fixation of the immobilization device, as well as a place for fixing the immobilization device; 4) Suitability of the immobilization device according to the animal's body, the device consists of a stainless steel mesh with a shape similar to a "T"; 5) Fixing the device, stage in which the lateral ends of the device are wrapped around the animal's body, fixed with the aid of adhesive tape and the spaces filled with cotton; 6) Immobilization, at this stage the device's fixation is inspected, in which the need for reinforcement with adhesive tape or filling with cotton is verified (20). After 10 days, the immobilization devices were removed, the animals in Group PI remained in their respective cages with free movement of the fore and hind limbs, while the animals in Group TI were subjected to vertical ladder training (21).

## Vertical ladder training

At 70 days of age, the animals in Group T and TI were subjected to the vertical ladder training protocol (110 × 18 cm, 2 cm grid, and 80° inclination), carried out on alternate days for 7 days, totaling up to 4 sessions. The sessions consisted of 9 climbs, with an interval of 60s, and without additional overload, just with a load of body mass (22). All sessions were held at the same time of day.

## Performance analysis

For performance analysis, the time of each climb and the number of grasping movements of the right forelimb were collected in each training session. The collected data were previously identified for non-normality using the Shapiro-Wilk Normality Test and analyzed using the Kruskal-Wallis test ($p < 0.05$) with the aid of GraphPad Prism 8®.

## Body mass

Using a semi-analytical scale (Marte LC1®), the body mass of the animals was measured at different periods: Pre-protocol, marked by the beginning of the muscular atrophy protocol for Groups I, PI, and TI; and 4 Collection Periods, delimited by the collection of biological material. After collecting the body mass data and identifying the non-normality of the data with the Shapiro-Wilk Normality Test, the Kruskal-Wallis statistical test ($p < 0.05$) was performed using the GraphPad Prism 8®.

## Muscle mass

After dissection, the mass of the gastrocnemius muscle was measured using a semi-analytical scale (Marte AD330). Using the data, the Shapiro-Wilk Normality Test was performed and the One-way ANOVA test ($p < 0.05$) was performed with the aid of GraphPad Prism 8®.

## Sample processing

For the dissection of the gastrocnemius muscle of the right hind limb, the animals were euthanized with an overdose of anesthetic (Ketamine 200 mg/kg and Xylazine 50 mg/kg). After dissection, the samples were smeared in neutral talc (Tragacanth®, SIGMA) to prevent artifacts, stabilized in cryomolds with biological glue (Tissue Tek®), cryofixed in liquid nitrogen -196 °C.

### Light microscopy

The belly samples (n = 5) were sectioned transversely (10 µm – Cryostat HM 505 E, MICROM®), placed on histological slides, and stained with Hematoxylin-Eosin (HE) to highlight cellular components, and Picro-Sirus Red (PSR) to identify intramuscular connective tissue (23, 24). The slides were analyzed and photographed with the aid of the Leica DM750® Light Microscope, at the Laboratory of Ecotoxicology and Conservation of Bees (LECA) - UNESP/ Rio Claro/SP.

### Fractal dimension

Using light micrographs, the Fractal Dimension (FD) of the nuclei and intramuscular connective tissue was analyzed with the help of ImageJ® Software. FD is a mathematical method in histological analyses, which measures the structural complexity of irregular geometric figures through similarity (25). This method is carried out through image binarization, in which all stained points in HE stains are identified in the images. The regression line generated from the number and sizes of squares necessary to cover the image results in a FD value (26, 27). The FD value is expressed on a scale of 0 to 2, where 0 indicates a lower stage of organizational complexity and 2 represents a higher stage (26). In addition to FD, with the binarization of PSR micrographs, it was possible to quantify the area of associated connective tissue using ImageJ® Software. 6 images/samples were selected with 20,000X magnification for each color, totaling 30 images/group/period, which were analyzed for the FD of the nucleus, and quantification of the intramuscular connective tissue area. After identifying non-normality using the Shapiro-Wilk Normality Test, the Kruskal-Wallis test ($p<0.05$) was performed using GraphPad Prism 8®.

### Myofibrillar ATPase

The belly samples (n = 5) were transversely sectioned (10 µm thick – Cryostat HM 505E, MICROM®), incubated for 30 min in a solution of 10 mg of ATP dissolved in distilled water with 10 ml of glycine/NaCl, $CaCl_2$ reaching pH 9.4 added with Dithiothreitol. Then, the sections were washed in distilled water and incubated for 7 min in 2% cobalt chloride, dehydrated in an increasing series of alcohols, and finished in xylene (22, 28). The images were obtained using the Leica DM750® Light Microscope, at the Laboratory of Ecotoxicology and Conservation of Bees (LECA) - UNESP - in Rio Claro/SP. From the micrographs, it was possible to differentiate and measure the cross-sectional area of type I and II muscle fibers. 100 fibers/group/period of each fiber type were randomly selected, with the help of ImageJ® Software. After obtaining the data, the non-normality of the data was identified using the Shapiro-Wilk Normality Test and then the Kruskal-Wallis test ($p < 0.05$) was performed using GraphPad Prism 8®.

## RESULTS

### Functional performance

In the 1st training session, Groups TI0h, TI4d, and TI7d showed greater time and number of movements ($p < 0.0001$) to perform the climbs, respectively compared to Group T0h, T4d, and T7d (**figure 1B,C**). In the 4th training session, Groups TI0h and TI24h did not demonstrate significant changes in time and movement ($p > 0.05$), while Groups TI4d and TI7d showed longer climbing time ($p < 0.0001$) respectively compared to the Groups T4d and T7d, however, no statistical changes in the number of movements ($p > 0.05$) (**figure 1D,E**).

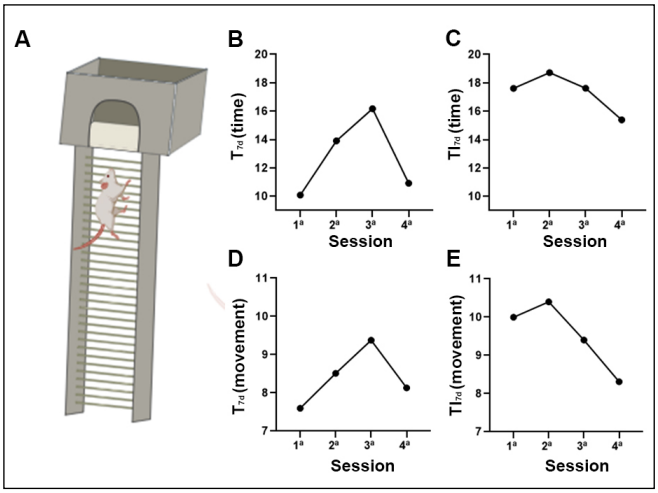


**Figure 1.** The functional analysis of the training was carried out by measuring **(A)** time and number of movements of the right forelimb used for each staircase; **(B)** Timing data from the T7d subgroup; **(C)** Timing data of the IT7d subgroup; **(D)** Movement data of subgroup T7d; **(E)** Motion data from the IT7d subgroup.

### Body Mass (BM)

Group C presented a higher body mass value ($p > 0.05$) when compared to P0h with the pre-protocols period. With training, a greater BM was observed in Groups T0h ($p > 0.05$), T24h ($p > 0.05$), T4d ($p > 0.05$), and T7d ($p > 0.05$) respectively about C, T0h T24h, and T4d. Immobilization

**Table I.** Body mass of the experimental groups.

| BM (g) | Pre-protocols | P0h | P24h | P4d | P7d |
|---|---|---|---|---|---|
| Control | 254.80 ± 19.25 | 287.40 ± 19.26 | - | - | - |
| Trained | 277.45 ± 17.72 | 322.00 ± 30.67 | 304.80 ± 12.76 | 314.60 ± 41.78 | 324.80 ± 37.32 |
| Immobilized | 248.90 ± 21.16 | 229.80 ± 25.46 | - | - | - |
| Post-immobilization | 248.90 ± 21.16 | - | 217.40 ± 16.01 | 260.40 ± 06.35 | 272.40 ± 27.19 |
| Trained immobilized | 246.65 ± 17.72 | 208.20 ± 17.95*** | 237.00 ± 14.09 | 251.00 ± 18.03 | 269.80 ± 17.91 |

Mean and standard deviations of body mass for all experimental groups; ***TI0h ≠ T0h $p < 0.001$.

(I0h, PI24h, PI4d, and PI7d) also did not result in statistically significant changes in the animals' body mass ($p > 0.05$). Training after muscular atrophy did not demonstrate significant changes in intra-group comparisons ($p < 0.05$). Regarding comparisons between groups, TI0h showed lower BM ($p < 0.001$) compared to T0h (**table I**).

## Muscle Mass (MM)

With training, MM values did not demonstrate significant changes in T0h, T24h, T4d, and T7d ($p > 0.05$) compared to Groups C, T0h, T24h, and T4d. Immobilization did not result in statistically significant adaptations when comparing Groups I0h, PI24h, PI4d, and PI7d ($p > 0.05$), despite the evolution of MM over the periods. The training intervention after muscular atrophy resulted in a progressive increase in MM values throughout the collection periods, with emphasis on TI4d ($p > 0.05$) which demonstrated significant changes about TI24h and TI7d ($p > 0.05$) compared to TI4d. However, when analyzing the MM of the groups submitted to the different protocols, Group T showed no changes ($p > 0.05$), while Group I0h demonstrated lower MM ($p < 0.0001$) concerning Group C. Likewise, Group TI0h, TI24h, TI4d and TI7d showed lower MM ($p < 0.0001$), respectively compared to T0h, T24h, T4d and T7d (**table II**).

## Nuclei disposition and tissue organization

In Group C, the distribution of polygonal-shaped muscle fibers was observed, organized in fascicles, with their nuclei arranged peripherally. Furthermore, in the interstitial space, the presence of blood vessels and a nerve bundle was observed (**figure 2C**).

The T0h Group presented muscle fibers with elongated and polygonal shapes and similar sizes, in addition to a uniform nuclear arrangement in the peripheral region. The vascularization and innervation structures are close together, with a greater presence of nuclei in the connective tissue adjacent to these structures (**figure 2 – T0h**).

In the T24h Group, the muscle fibers have rounded and elongated shapes, with their nuclei peripheral. Blood vessels were observed spaced along the perimysium with greater adjacent nuclear presence. Highlighted, the arteries demonstrate oblique dispositions, evidenced by the absence of the lumen and striations (**figure 2 – T24h**).

The T4d Group demonstrates wide adaptation in the sizes of muscle fibers, in which the smaller fibers have a rounded shape, and the larger ones have a polygonal and elongated shape. The nuclei were observed peripherally and spacing in the larger fibers, opposing nuclear condensation in the smaller fibers. Vascular and nervous

**Table II.** Mean and standard deviations of gastrocnemius muscle mass.

| MM (g) | P0h | P24h | P4d | P7d |
|---|---|---|---|---|
| Control | 1.383 ± 0.10 | - | - | - |
| Trained | 1.548 ± 0.25 | 1.434 ± 0.15 | 1.491 ± 0.19 | 1.578 ± 0.14 |
| Immobilized | 0.654 ± 0.32**** | - | - | - |
| Post-immobilization | - | 0.624 ± 0.13 | 0.804 ± 0.07 | 0.933 ± 0.09 |
| Trained Immobilized | 0.688 ± 0.10*** | 0.710 ± 0.15**** | 0.807 ± 0.04**** | 1.008 ± 0.07**** |

****I0h ≠ C $p < 0.0001$; TI0h ≠ T0h $p < 0.0001$; TI24h ≠ T24h $p < 0.0001$; TI4d ≠T4d $p < 0.0001$; TI7d ≠ T7d $p < 0.0001$.

structures have a close relationship. (**figure 2 – T4d**).
In Group T7d, fibers were found with similar sizes and shapes and nuclei spaced around their periphery. In the adjacent connective tissue, the vascular and nervous structures showed a higher nuclear concentration, especially the arteries nearby, due to their "united" arrangement (**figure 2 – T7d**).
In Group I0h, the fibers demonstrate changes in shape (elongated, oval, and polygonal) resulting from muscle atrophy. In a close relationship, the vascularization structures and the nerve fiber bundle were observed, in addition to a greater nuclear concentration in the large area of associated connective tissue (**figure 2 – I0h**).
After 24 hours, it is noted in the PI24h Group that the muscle fibers maintain their distinct shapes, however, with an extensive nuclear presence in the periphery. The extracellular matrix region shows blood vessels and nerve bundles (**figure 2 – PI24h**).
The PI4d Group presents maintenance of irregular muscle fiber shapes, with extensive spacing between muscle bundles. Meanwhile, the largest area of vascular and nervous structures stands out for its arrangement along several fascicles and with three bundles of nerve fibers in their different diameters, in addition to a less accentuated concentration of adjacent connective tissue nuclei (**figure 2 – PI4d**).
In Group PI7d, there is greater uniformity in muscle fibers, in their sizes and rounded shapes. In some regions, nuclear condensations were evident with peripheral nuclei and centralized muscle fibers. Furthermore, the association of vas-

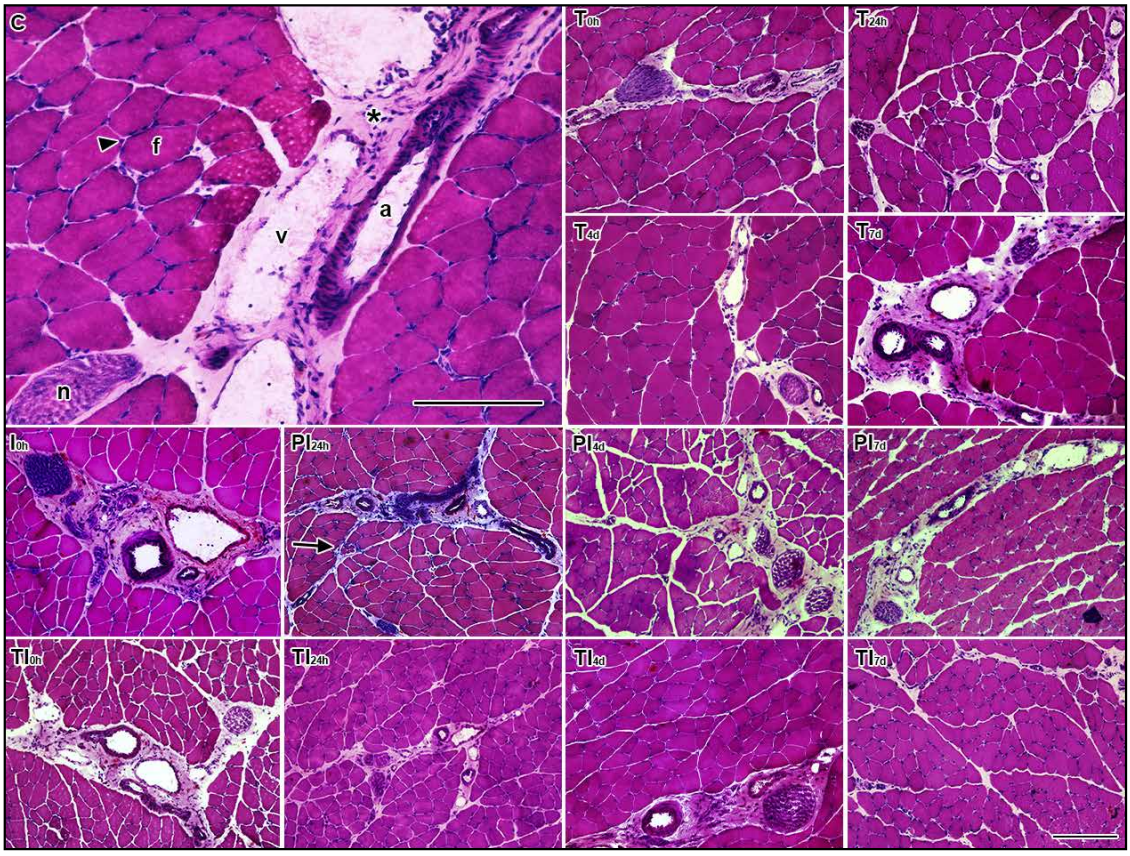


**Figure 2.** Light Microscopy with Hematoxylin and Eosin staining of all Experimental Groups, which allowed the identification of muscle fibers **(f)** with their peripheral nuclei (arrowhead), in addition to the arrangement of vascular structures, such as arterioles **(a)** and venules **(v)**, and nervous structures, such as the nerve fiber bundle **(n)** and the neuromuscular spindle (arrow), arranged in a wide area of connective tissue (*) in the interstitial space.

Experimental Groups: Control (C), Trained 0 hours (T0h), Trained 24 hours (T24h), Trained 4 days (T4d), Trained 7 days (T7d), Immobilized 0 hours (I0h), Post-Immobilization 24 hours (PI24h), Post-Immobilization 4 days (PI4d), Post-Immobilization 7 days (PI7d), Trained Immobilized 0 hours (TI0h), Trained Immobilized 24 hours (TI24h), Trained Immobilized (TI4d), Trained Immobilized 7 days (TI7d). Magnifications: 20000x. Bars: 100 µm.

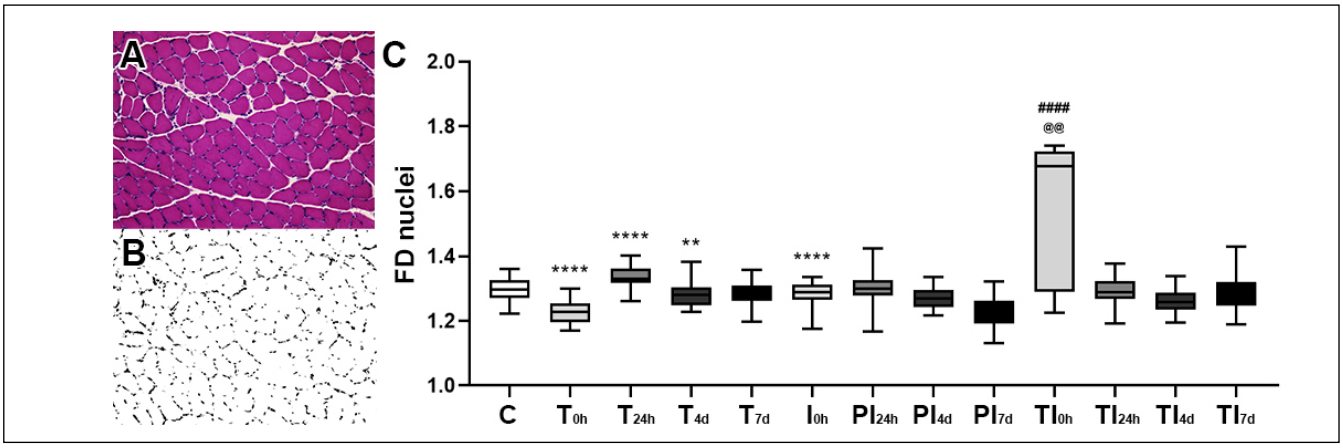


**Figure 3.** Micrograph stained with Hematoxylin and Eosin **(A)** were analyzed using the binarization tool **(B)**. The organization complexity of the muscle fiber nuclei of all experimental groups **(C).**

Groups: Control (C), Trained 0 hours (T0h), Trained 24 hours (T24h), Trained 4 days (T4d), Trained 7 days (T7d), Immobilized 0 hours (I0h), Post-Immobilization 24 hours (PI24h), Post-Immobilization 4 days (PI4d), Post-Immobilization 7 days (PI7d), Trained Immobilized 0 hours (TI0h), Trained Immobilized 24 hours (TI24h), Trained Immobilized (TI4d), Trained Immobilized 7 days (TI7d). Magnifications (A, B): 20000X. T0h ≠ C ($p < 0.0001$); T24h ≠ T0h ($p < 0.0001$); T4d ≠ T24h ($p < 0.01$); TI0h ≠ T0h ($p < 0.0001$); TI0h ≠ I0h ($p < 0.01$).

cular and nervous structures, in a wide area of connective tissue (**figure 2 – PI7d**).

Finally, in the TI0h Group, irregular shapes (oval and elongated) of the muscle fibers were observed, with their peripheral nuclei. The vascular structures were found with greater density and proximity, with emphasis on the arrangement of the arteries. In addition to the presence of a nerve fiber bundle (**figure 2 – TI0h**).

After 24 hours, the TI24h Group presented muscle fibers with an irregular shape, and an extensive concentration of nuclei in their periphery, with reorganization of the fascicles. Blood vessels and nerve fiber bundles demonstrate greater density and spaced arrangement in the perimysium along several fascicles. A neuromuscular spindle was also found nearby (**figure 2 – TI24h**).

In Group TI4d, muscle fibers with different shapes and diameters were observed. In the interstitial space, the blood vessels and nerve fiber bundle are closer and have a higher nuclear concentration (**figure 2 – TI4d**).

The TI7d Group presents muscle fibers with irregular diameters, polygonal and elongated shapes, with irregularly arranged peripheral nuclei, in addition to some regions of nuclear condensation. In the perimysium, blood vessels and bundles of nerve fibers were observed spaced along several fascicles (**figure 2 – TI7d**).

## Nuclei complexity

Vertical ladder training caused lower organizational complexity in T0h ($p < 0.0001$) concerning Group C, while T24h demonstrated greater organizational complexity compared to T0h ($p < 0.0001$), and lower organizational complexity in T4d ($p < 0.01$) about T24h. In Group T7d there were no significant adaptations ($p > 0.05$) compared to other groups (**figure 3C**).

Immobilization Groups I0h, PI24h, PI4d, and PI7d did not demonstrate statistically significant changes ($p > 0.05$) respectively in comparison to Groups I0h, PI24h, and PI4d (**figure 3C**).

With the training intervention after muscular atrophy, TI0h showed greater complexity in the organization of the nuclei, both in comparison to I0h ($p < 0.05$) and with T0h ($p < 0.0001$) (**figure 3C**). However, Groups TI24h, TI4d and TI7d did not reveal statistical differences compared to Groups PI24h, PI4d, PI7d, T24h, T4d and T7d ($p>0.05$) (**figure 3C**).

## Intramuscular collagen deposition

In Group C, the intramuscular connective tissue was evidenced by a reddish color, in which it was possible to identify the perimysium surrounding the muscle fascicles and the endomysium surrounding the muscle fibers (**figure 4C**).

The T0h Group showed the perimysium around the muscle fascicles, as well as the endomysium surrounding the muscle fibers (**figure 4 – T0h**). In Group T24, the perimysium surrounding the fascicles and the endomysium surrounding the muscle fibers were intensified by the reddish color (**figure 4 – T24h**). Group T4d demonstrated more discrete identification of the perimysium and endomysium, respectively,

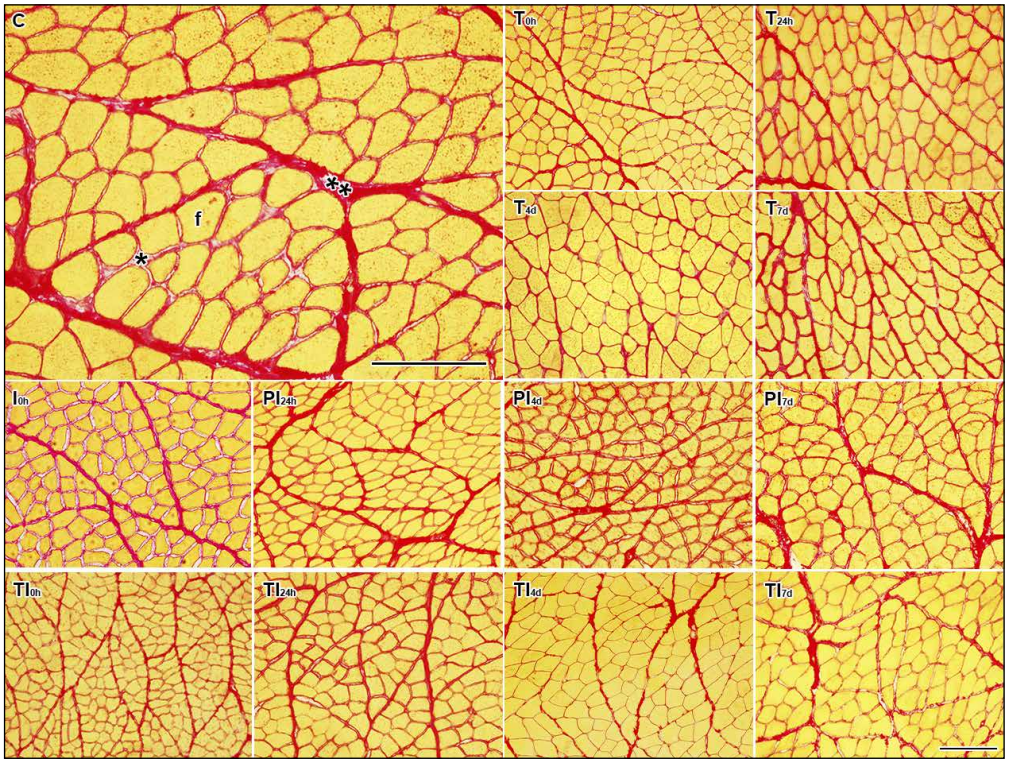


**Figure 4.** Light Microscopy with Picrosirius Red staining from the Experimental Groups, to identify the muscle fibers **(f)** with the endomysium (*) surrounding the muscle fibers and the perimysium (**) involving a bundle of fibers, of all the Experimental Groups.

Groups: Control (C), Trained 0 hours (T0h), Trained 24 hours (T24h), Trained 4 days (T4d), Trained 7 days (T7d), Immobilized 0 hours (I0h), Post-Immobilization 24 hours (PI24h), Post-Immobilization 4 days (PI4d), Post-Immobilization 7 days (PI7d), Trained Immobilized 0 hours (TI0h), Trained Immobilized 24 hours (TI24h), Trained Immobilized (TI4d), Trained Immobilized 7 days (TI7d). Magnifications: 200x. Bars: 100 µm.1).

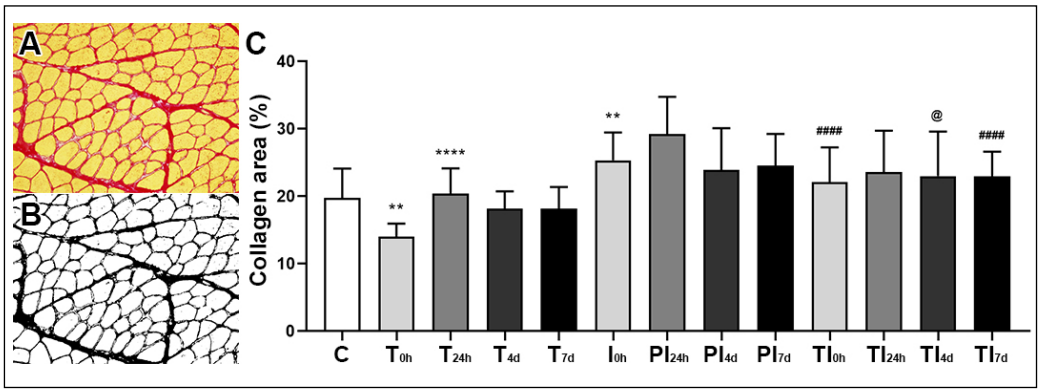


**Figure 5.** Quantification of the area of collagen connective tissue in Picro Sirius-Red micrographs **(A)** performed through binarization **(B)**. (Collagen Area %) Experimental Groups.

Groups: Control (C), Trained 0 hours (T0h), Trained 24 hours (T24h), Trained 4 days (T4d), Trained 7 days (T7d), Immobilized 0 hours (I0h), Post-Immobilization 24 hours (PI24h), Post-Immobilization 4 days (PI4d), Post-Immobilization 7 days (PI7d), Trained Immobilized (TI0h), Trained Immobilized 24 hours (TI24h), Trained Immobilized (TI4d), Trained Immobilized 7 days (TI7d). Magnifications (A, B): 20000X. T0h ≠ C ($p < 0.01$); T24h ≠ T0h ($p < 0.0001$); I0h ≠ C ($p < 0.01$); TI0h ≠ T0h ($p < 0.0001$); TI4d ≠ PI4d ($p < 0.05$); TI7d ≠ T7d ($p < 0.0001$).

around the fascicles and muscle fibers (**figure 4 – T4d**). In Group T7d, there was also clear evidence of the perimysium involving the fascicles and the endomysium surrounding the muscle fibers (**figure 4 – T7d**).

Group I0h revealed adaptations with the identification of the perimysium in the reddish color around the muscle fascicles, with a reduction in the identification of the endomysium (**figure 4 – I0h**). After 24 hours, in the PI24h Group, the presence of smaller muscle fascicles was observed, which allowed better identification of the perimysium, while the endomysium demonstrated identification around the muscle fibers (**figure 4 – PI24h**). In Group PI4d, the perimysium and endomysium were well identified by the reddish color, respectively surrounding the fascicles and muscle fibers (**figure 4 – PI4d**). The PI7d Group revealed better identification of the perimysium around the fascicles, and discrete identification of the endomysium surrounding the muscle fibers (**figure 4 – PI7d**).

The TI0h Group demonstrated the presence of smaller fascicles with better identification of the perimysium due to the reddish color, in addition to the endomysium surrounding the muscle fibers (**figure 4 – TI0h**). After 24 hours, the TI24h Group also revealed better identification of the perimysium around the fascicles, as well as the endomysium surrounding the muscle fibers (**figure 4 – TI24h**). In Group TI4d, it was possible to identify the perimysium and endomysium, respectively, around the fascicles and muscle fibers (**figure 4 – TI4d**). P7d from Group TI7d showed better evidence of the perimysium due to its reddish color, in addition to more discreet identification of the endomysium surrounding the muscle fibers (**figure 4 – TI7d**).

### Intramuscular connective tissue area

Training resulted in a smaller connective tissue area ($p < 0.01$) in Group T0h compared to Group C, while T24h presented a larger connective tissue area ($p < 0.001$) compared to T0h. However, Groups T4d and T7d did not reveal statistical differences ($p > 0.05$) (**figure 5C**).

Quantification of the connective tissue area after immobilization demonstrated a greater area in Group I0h ($p < 0.01$) concerning C. While Groups PI24h, PI4d, and PI7d did not demonstrate significant adaptations ($p > 0.05$) (**figure 5C**).

The TI0h Group revealed a greater area of connective tissue ($p < 0.0001$) compared to T0h, as well as in TI7d, there was a greater area of connective tissue ($p < 0.05$) compared to T7d. TI24h and TI4d did not show statistical changes, respectively, for Groups T24h and T4d. In comparison to the groups subjected to immobilization, in Group TI4d a larger area ($p < 0.05$) was observed about PI4d, while in Groups I0h, PI24h, and PI7d ($p > 0.05$) (**figure 5C**).

### Cross Section Area (CSA) remodeling

With training, both type I fibers and type II fibers showed no changes in T0h compared to Group C, as well as in T24h, T4d, and T7d respectively about T0h, T24h, and T4d ($p > 0.05$) (**figure 6B,C**).

Immobilization resulted in a decrease in the area in type I ($p < 0.0001$) and II ($p < 0.0001$) fibers in I0h concerning Group C, as well as in PI24h there was a lower CSA in type I fibers ($p < 0.001$) and II ($p < 0.001$) compared to I0h. While PI7d demonstrated higher CSA of type I ($p < 0.0001$), and II ($p < 0.01$) fibers compared to PI4d (**figure 6B,C**).

The TI Group demonstrated higher CSA of type I and II fibers in TI7d ($p < 0.0001$) rather than TI4d. The remaining intragroup comparisons did not show statistically significant changes ($p > 0.05$) (**figure 6B,C**).

In comparison to the groups subjected to training, TI0h demonstrated lower CSA in type I ($p < 0.0001$) and type II ($p < 0.0001$) fibers compared to T0h. In TI24h, there was a decrease in the area in type I ($p < 0.0001$) and II ($p < 0.0001$) fibers compared to T24h. TI4d demonstrated lower CSA of type I ($p < 0.0001$), and II ($p < 0.0001$) fibers compared to T4d. In TI7d, lower CSA was observed in type I ($p < 0.0001$) and II ($p < 0.0001$) fibers to T7d (**figure 6B,C**).

Compared to the immobilized Groups, the TI0h Group presented lower CSA type I ($p < 0.0001$) and II ($p < 0.0001$) fibers concerning the I0h. While the other comparisons of TI24h, TI4d, and TI7d did not reveal statistical differences compared to Groups PI24h, PI4d, and PI7d (**figure 6B,C**).

## DISCUSSION

The present study showed the acute adaptations of the structural components of the muscle belly after using training as an intervention for the harmful repercussions caused by muscular atrophy, highlighting the monitoring of the initial changes in each structure. This provides new evidence to elucidate the uniqueness adaptation of skeletal striated muscle to resistance training without additional load.

The use of chronic training to reverse the harmful effects of atrophy has been proven to be effective in several studies (29-32). Among the repercussions of atrophy attenuated by training, the functional capacity of the muscle is reduced, due to muscle stiffness caused by the overexpression of collagen, also known as fibrosis (33). Thus, the greater time and number of movements in the TI Group compared to the T Group is explained by the reduction in muscle extensibility that affects less joint mobility.

The focus of this work involves the adaptations that precede

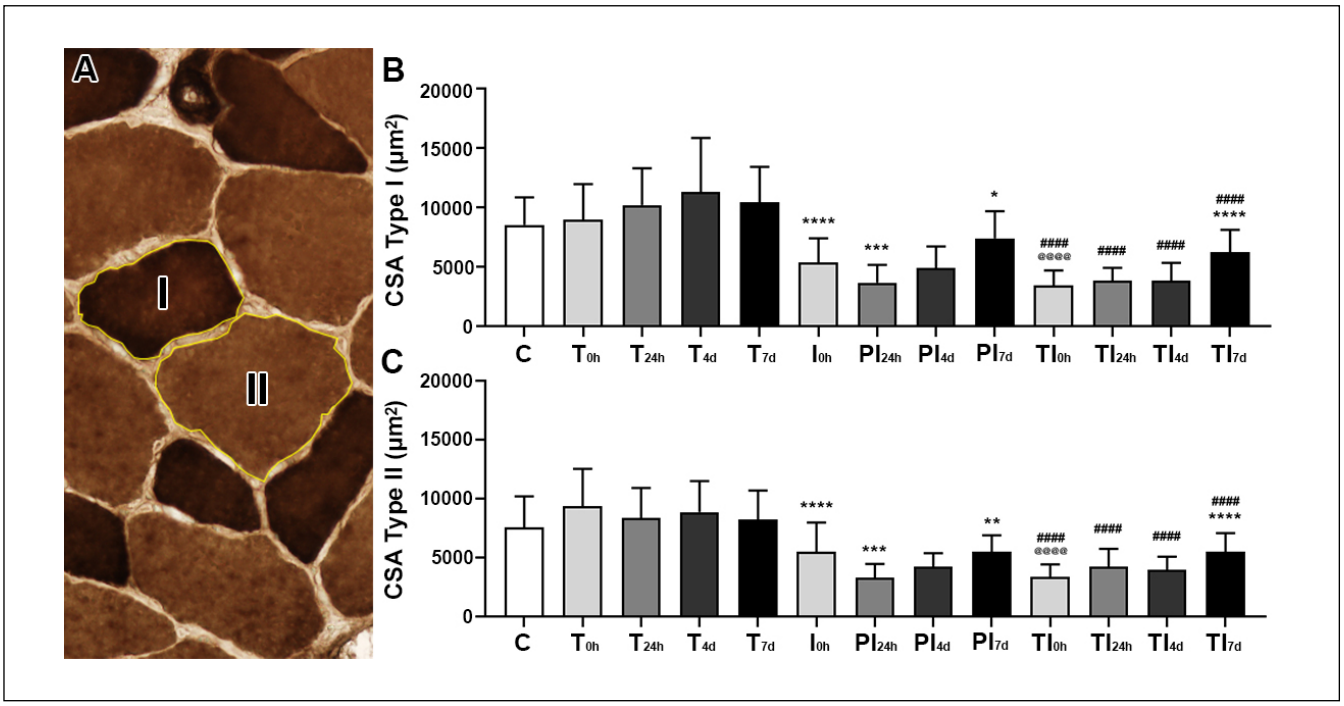


**Figure 6.** Cross-sectional area (CSA) of type I **(I)** and type II **(II)** muscle fibers performed using ATPase 9.4 **(A)** of all Experimental Groups.
Groups: Control (C), Trained 0 hours (T0h), Trained 24 hours (T24h), Trained 4 days (T4d), Trained 7 days (T7d), Immobilized 0 hours (I0h), Post-Immobilization 24 hours (PI24h), Post-Immobilization 4 days (PI4d), Post-Immobilization 7 days (PI7d), Trained Immobilized 0 hours (TI0h), Trained Immobilized 24 hours (TI24h), Trained Immobilized (TI4d), Trained Immobilized 7 days (TI7d). Magnification: 400X. Fiber type I: I0h ≠ C ($p < 0.0001$); PI24h ≠ I0h ($p < 0.001$); PI7d ≠ PI4d ($p < 0.0001$); TI0h ≠ T0h ($p < 0.0001$); TI0h ≠ I0h ($p < 0.0001$); TI24h ≠ T24h ($p < 0.0001$); TI4d ≠ T4d ($p < 0.0001$); TI7d ≠ TI4d ($p < 0.0001$); TI4d ≠ T4d ($p < 0.0001$). Fiber type II: I0h ≠ C ($p < 0.0001$); PI24h ≠ I0h ($p < 0.001$); PI7d ≠ PI4d ($p < 0.01$); TI0h ≠ T0h ($p < 0.0001$); TI0h ≠ I0h ($p < 0.0001$); TI24h ≠ T24h ($p < 0.0001$); TI4d ≠ T4d ($p < 0.0001$); TI7d ≠ TI4d ($p < 0.0001$); TI4d ≠ T4d ($p < 0.0001$).

the muscle regeneration process, both in a healthy environment and in an environment impaired by muscular atrophy. Therefore, muscle mass was evaluated to determine the effectiveness of the experimental model chosen to trigger atrophy. Joint immobilization for 10 days resulted in a reduction in muscle mass by 47% (I0h), which corroborates Kim *et al.* (2018) description of an extensive decrease in the gastrocnemius muscle of immobilized *Wistar* rats (34).
Joint immobilization causes muscle atrophy through inactivity, since prolonged periods of disuse result in the loss of mass in isolated muscle groups (35). During the period of return from mechanical load, there is an increase in reactive oxygen species in the mitochondria, which causes mitochondrial dysfunction and inflammation, in addition to regulating autophagy through the ubiquitin-proteasome system until the initial 7 days of remobilization in an experimental model (36, 37). In our data, we observed lower muscle mass in the initial periods of remobilization (I0h and PI24h) after 10 days of immobilization, which corroborates the worsening of muscle atrophy in the acute period.
The atrophic ubiquitin-proteasome pathway is regulated by MURF-1 and Atrogin-1, which is responsible for exacerbated proteolysis. After a moderate training session, the protein content of MURF-1 decreases, however after 6 hours the content increases again (34, 38). The lower mass of the gastrocnemius muscle at T0h, as well as the progressive increase in muscle mass at T24h, T4d, and T7d can be explained by the momentary reduction in atrophic pathways and an increase in hypertrophic pathways.
A geometric method that stands out in the scientific field is FD, due to its effectiveness in quantifying the architecture of different tissues, as it allows the measurement of the structures of a tissue as a whole, in addition to standardizing the measurement of binarized points, which reduce manual quantification errors (39). Tissue remodeling is demonstrated by changes in structures, thus adaptations in shape,

density, and arrangement can affect the architecture of this tissue, which is represented by FD (26).

In HE stains, the nuclei are evident, without distinction between cell nuclei (*i.e.*, fibroblasts and satellite cells) (40). Thus, the lower complexity of the organization immediately after a training session (T0h) may indicate the dynamic remodeling of the nuclei, since an increase in the FD value is then observed at T24h, T4d, and T7d. Our findings correlate with Von Walden *et al.* (2020) lower proportion of myonuclei as an acute response to resistance training, which indicates the acute proliferation and infiltration of cells mediated by training as responsible for the increased levels of nuclei (40, 41).

Myonuclei play a fundamental role in transcriptional coordination, in which their peripheral location allows strategic positioning close to the plasma membrane and the center of the muscle fiber, facilitating communication and transcriptional transport (17, 42). Atrophic conditions disturb the myonuclear arrangement due to grouping, since some myonuclei come closer together and give rise to spaces, called by Hannson *et al.* (2020) as gaps. These imply large cytoplasmic volumes per nucleus that affect activities of transcriptional and protein synthesis, resulting in the physiological deterioration of muscle fibers through myonuclear dysfunction (42). Specifically in FD, the lower complexity of organization observed after immobilization for 10 days (I0h), indicates the relationship with the myonuclear grouping that alters the arrangement and suggests the impairment of myonuclear function.

Resistance training is used to establish a favorable environment for muscle hypertrophy, in which myonuclear growth is one of the essential adaptations for the growth of muscle fibers. The immediate return of mechanical load through 1 session of resistance training resulted in a higher FD value, which implies greater organization of myonuclei, due to the adaptations that resistance training causes in myonuclear quantity and the expansion of its domains (43).

The adaptive characteristic of intramuscular connective tissue is of notable relevance for several studies, due to its contribution to the communication of other cells (*i.e.*, satellite cells) that provide support for musculoskeletal remodeling (44). Acute resistance training triggers the formation of a transition matrix from a rapid catabolic process that precedes the anabolic processes, just as we observed the smallest area of connective tissue immediately after 1 training session (T0h), while in the other periods analyzed (T24h, T4d, and T7d). There was an increase in the area of connective tissue, which corroborates the rapid activation of collagen synthesis pathways that occur intending to reinforce the structure of this tissue (5).

In addition to its unique characteristic in remodeling, connective tissue has a network-like arrangement around muscle fibers, thereby providing mechanical support for other structures, such as blood vessels and nerves (45). Excessive deposition and disorganized arrangement of collagen fibers are widely reported with muscle atrophy, and the main consequences surrounding this remodeling are a decrease in blood supply at the capillary level and an increase in the stiffness of muscle tissue (46, 47). Therefore, the increase in the positive area of connective tissue after 10 days of joint immobilization (I0h) negatively reflects on the integrity of the blood supply and the contractile properties of the gastrocnemius muscle.

The composition of intramuscular connective tissue in the face of immobilization portrays the negative remodeling of this tissue, since immobilization intensifies the synthesis and irregular arrangement of collagen types I and III, responsible for the formation of collagen fibrils. In addition to reducing the synthesis of collagen type V, which acts as the main component of the basement membrane, together these adaptations impact the rigidity and vulnerability of this tissue (45, 48, 49). Therefore, the exacerbated presence of connective tissue observed with immobilization (I0h) denotes a weakened tissue, which affects the structural and functional quality of the muscle tissue as a whole.

Contrary to the expectations of numerous studies, the interruption of atrophic stimuli does not attenuate disturbed remodeling of the components of the muscular connective tissue, as the continuous process of synthesis and disorganization of collagen fibers is reported (48). These data corroborate our findings, in which 24 hours after the end of the atrophy protocol (PI24h). There is a marked increase in the area of connective tissue concerning the immediate period after the immobilization device was removed, and consequently predicts the fragility of this tissue in the acute period of remobilization.

Resistance training quickly triggers (1-6 hours) changes in the expression levels of genes involved in renewing the structure and composition of intramuscular connective tissue components (44). The interruption of the harmful process that results in muscle stiffness after training has a positive impact on the functional point of view of skeletal striated muscle. Stiffness of the non-contractile tissue impairs the radial expansion of muscle fibers, and consequently affects shortening during training. Concentric contraction of resistance training (50). Therefore,

the smaller positive area of collagen in Group TI0h and TI24h compared to Group I indicates the effectiveness of resistance training in inhibiting the progression of changes that result in structural and functional fragility of intramuscular connective tissue.

The training protocol used was resistance training carried out with the aid of a vertical ladder, chosen based on the principles of reproducibility, an experimental protocol similar to intervention protocols for muscular atrophy in humans; movement technique, concentric and eccentric contractions; result, a protocol with a chronic effect on muscle hypertrophy proven in the literature. However, in our study, the training was implemented without additional load on body mass, and the acute repercussions were analyzed. Therefore, the statistically insignificant changes observed in the T0h, T24h, T4d, and T7d Groups indicate the initial development of muscular hypertrophy that manifests marked adaptations after 2-3 weeks of training (51).

The mechanical load caused by muscle contraction results in the activation of pathways that affect various signaling processes that inhibit catabolic pathways and regulate mitochondrial biogenesis and renewal. The extracellular redox consequently reduces the production of reactive oxygen species and positively regulates antioxidant enzymes. On the other hand, the mechanical discharge caused by immobilization implies a disturbed homeostatic state due to the fission of the mitochondrial membrane, hyperactivation of the ubiquitin-proteasome system pathways, and other pathways that result in an increase in reactive oxygen species, in addition to the production and secretion of cytokines. Pro-inflammatory, which implies oxidative stress (52).

In the present study, joint immobilization results in a marked reduction in the CSA of type I and II muscle fibers (I0h), which corroborates the findings of other studies that reported muscle atrophy caused by the suspension of the lower limbs, immobilization by plaster and cachexia (35, 53-55). The smaller cross-sectional area of muscle fibers directly implies force production, therefore, our findings predict a reduction in muscle strength in *Wistar* rats immobilized for 10 days (I0h).

However, the interruption of the absence of load is not accompanied by the absence of continuity in the transverse reduction of muscle fibers. As was observed in our study, type I and II muscle fibers demonstrated a notable reduction in CSA after 24 hours with free movement of the previously immobilized hind limb.

From a morphological point of view, the composition of the muscle fiber can be understood as myofibrillar and protein fractions. The myofibrillar fraction corresponds to the majority of the fiber, formed by numerous myofibrillar proteins (*i.e.*, myosin, actin, troponin, alpha-actin, myopalladin, myomesin, titin, nebulin, among others). While the sarcoplasmic fraction is made up of sarcoplasm, organelles, cellular components (*i.e.*, mitochondria and sarcoplasmic reticulum), macromolecules (*i.e.*, ribosomes, glycogen, and lipid droplets), and enzymes (56). Therefore, skeletal striated muscle can present two types of hypertrophy: myofibrillar, radial growth through the proportional increase of proteins and sarcoplasmic space; and sarcoplasmic, expansion of sarcoplasmic content accompanied by an increase in the volume of organelles arranged in the sarcoplasm (57).

Sarcoplasmic hypertrophy is described as a stage that precedes myofibrillar hypertrophy and is thus established as a transient process, which indicates the beginning of remodeling of muscle tissue towards radial and sarcomeric growth of muscle fibers (56, 58). From this, we postulate that the initial increase in type I and II fibers by resistance training after muscle atrophy (TI0h and TI24h) results from the expansion of non-myofibrillar components. Our findings are supported by Burd *et al.* (2010) who described resistance training as stimulating the synthesis of sarcoplasmic proteins after 4 and 24 hours of the session (59).

### Limitations of the study

The present study showed the morphological perspective of immobilization and vertical ladder training and demonstrated the nuclear and connective tissue aspects associated with the adaptations of fiber types. For greater specificity of adaptations, molecular analyses regarding the types of collagens, nuclear proteins of the muscle and extracellular matrix, and proteins associated with muscle fibers must be carried out related to these protocols.

## CONCLUSIONS

We conclude that resistance training promoted changes in the arrangement and quantity of myonuclei in the muscle belly expanded the myonuclear domains and functionally supported the muscle fibers; accumulation of connective tissue extracellular matrix components indicates the presence of the transient matrix of non-contractile components that precede muscle regeneration; increase in CSA of muscle fibers since the 1st session inhibits the progression of atrophic effects even after interruption of the atrophy protocol.

## FUNDINGS

This work was financed by the Pro-Rectory of Post-Graduate Studies in partnership with the Pro-Rectory of Undergraduate Studies at São Paulo State University, which provided financial assistance (Notice 23/2022).

## DATA AVAILABILITY

Data are available under reasonable request to the corresponding author.

## CONTRIBUTIONS

BACG, APC: conceptualization. BACG, ANT, JRRS: methodology. BACG: data analysis/software and description of results. BACG, ANT, JPN, JRRS, APC: formal analysis. APC: resources, supervision, funding acquisition. BACG: writing the original draft. BACG, ANT; JPN, JRRS, APC: writing – review & editing.

## CONFLICT OF INTERESTS

The authors declare that they have no conflict of interests.

## REFERENCES

1. Mukund K, Subramaniam S. Skeletal muscle: A review of molecular structure and function, in health and disease. Wiley Interdiscip Rev Syst Biol Med. 2020;12(1):e1462. doi: 10.1002/wsbm.1462.
2. Qaisar R, Bhaskaran S, Van Remmen H. Muscle fiber type diversification during exercise and regeneration. Free Radic Biol Med. 2016;98:56-67. doi: 10.1016/j.freeradbiomed.2016.03.025.
3. Viggars MR, Wen Y, Peterson CA, Jarvis JC. Automated cross-sectional analysis of trained, severely atrophied, and recovering rat skeletal muscles using MyoVision 2.0. J Appl Physiol (1985). 2022;132(3):593-610. doi: 10.1152/japplphysiol.00491.2021
4. Kaczmarek A, Kaczmarek M, Ciałowicz M, et al. The Role of Satellite Cells in Skeletal Muscle Regeneration-The Effect of Exercise and Age. Biology (Basel). 2021;10(10):1056. doi: 10.3390/biology10101056.
5. Csapo R, Gumpenberger M, Wessner B. Skeletal Muscle Extracellular Matrix - What Do We Know About Its Composition, Regulation, and Physiological Roles? A Narrative Review. Front Physiol. 2020;11:253. doi: 10.3389/fphys.2020.00253.
6. Williams K, Yokomori K, Mortazavi A. Heterogeneous Skeletal Muscle Cell and Nucleus Populations Identified by Single-Cell and Single-Nucleus Resolution Transcriptome Assays. Front Genet. 2022;13:835099. doi: 10.3389/fgene.2022.835099.
7. Brooks NE, Myburgh KH. Skeletal muscle wasting with disuse atrophy is multi-dimensional: the response and interaction of myonuclei, satellite cells and signaling pathways. Front Physiol. 2014;5:99. doi: 10.3389/fphys.2014.00099.
8. Mikkelsen UR, Agergaard J, Couppé C, et al. Skeletal muscle morphology and regulatory signalling in endurance-trained and sedentary individuals: The influence of ageing. Exp Gerontol. 2017;93:54-67. doi: 10.1016/j.exger.2017.04.001.
9. Kunz RI, Coradini JG, Soares CLR, Brancalhão RMC, Bertolini GRF, Ribeiro L de FC. Efeitos da imobilização e remobilização pela combinação natação e salto em meio aquático, sobre a morfologia do músculo tibial anterior de ratos. Publicatio UEPG: Ciências Biológicas e da Saúde. 2013;19(2):123-9.
10. Fan Z, Xiao Q. Impaired autophagic flux contributes to muscle atrophy in obesity by affecting muscle degradation and regeneration. Biochem Biophys Res Commun. 2020;525(2):462-8. doi: 10.1016/j.bbrc.2020.02.110.
11. Barker RG, Wyckelsma VL, Xu H, Murphy RM. Mitochondrial content is preserved throughout disease progression in the mdx mouse model of Duchenne muscular dystrophy, regardless of taurine supplementation. Am J Physiol Cell Physiol. 2018;314(4):C483-91. doi: 10.1152/ajpcell.00046.2017.
12. Wilburn D, Ismaeel A, Machek S, Fletcher E, Koutakis P. Shared and distinct mechanisms of skeletal muscle atrophy: A narrative review. Ageing Res Rev. 2021;71:101463. doi: 10.1016/j.arr.2021.101463.
13. Bodine SC. The role of mTORC1 in the regulation of skeletal muscle mass. Fac Rev. 2022;11:32. doi: 10.12703/r/11-32.
14. Yin L, Li N, Jia W, et al. Skeletal muscle atrophy: From mechanisms to treatments. Pharmacol Res. 2021;172:105807. doi: 10.1016/j.phrs.2021.105807.
15. Yoshihara T, Sugiura T, Miyaji N, et al. Effect of a combination of astaxanthin supplementation, heat stress, and intermittent reloading on satellite cells during disuse muscle atrophy. J Zhejiang Univ Sci B. 2018;19(11):844-852. doi: 10.1631/jzus.B1800076.
16. Henriquez-Olguin C, Meneses-Valdes R, Jensen TE. Compartmentalized muscle redox signals controlling exercise metabolism - Current state, future challenges. Redox Biol. 2020;35:101473. doi: 10.1016/j.redox.2020.101473.
17. Hansson KA, Eftestøl E. Scaling of nuclear numbers and their spatial arrangement in skeletal muscle cell size regulation. Mol Biol Cell. 2023;34(8):pe3. doi: 10.1091/mbc.E22-09-0424.
18. Furrer R, Heim B, Schmid S, et al. Molecular control of endurance training adaptation in male mouse skeletal muscle. Nat Metab. 2023;5(11):2020-35. doi: 10.1038/s42255-023-00891-y.
19. Furlanetto R Jr, de Paula Souza A, de Oliveira AA, et al. Acute resistance exercise reduces increased gene expression in muscle atrophy of ovariectomised arthritic rats. Prz Menopauzalny. 2016;15(4):193-201. doi: 10.5114/pm.2016.65663.
20. Coutinho EL, Gomes AR, Franca CN, Salvini TF. A new model for the immobilization of the rat hind limb. Braz J Med Biol Res. 2002;35(11):1329-32. doi: 10.1590/s0100-879x2002001100010.
21. Rocha LC, Jacob CDS, Barbosa GK, et al. Remodeling of the skeletal muscle and postsynaptic component after short-term

joint immobilization and aquatic training. Histochem Cell Biol. 2020;154(6):621-8. doi: 10.1007/s00418-020-01910-9.
22. Rocha LC, Pimentel Neto J, de Sant'Ana JS, et al. Repercussions on sarcomeres of the myotendinous junction and the myofibrillar type adaptations in response to different trainings on vertical ladder. Microsc Res Tech. 2020;83(10):1190-7. doi: 10.1002/jemt.23510.
23. Cardiff RD, Miller CH, Munn RJ. Manual hematoxylin and eosin staining of mouse tissue sections. Cold Spring Harb Protoc. 2014;2014(6):655-658. doi: 10.1101/pdb.prot073411.
24. Bhutda S, Surve MV, Anil A, et al. Histochemical Staining of Collagen and Identification of Its Subtypes by Picrosirius Red Dye in Mouse Reproductive Tissues. Bio Protoc. 2017;7(21):e2592. doi: 10.21769/BioProtoc.2592.
25. Karperien A, Jelinek HF, Leandro JJ, Soares JV, Cesar RM Jr, Luckie A. Automated detection of proliferative retinopathy in clinical practice. Clin Ophthalmol. 2008;2(1):109-22. doi: 10.2147/opth.s1579.
26. Cury SS, Freire PP, Martinucci B, et al. Fractal dimension analysis reveals skeletal muscle disorganization in mdx mice. Biochem Biophys Res Commun. 2018;503(1):109-15. doi: 10.1016/j.bbrc.2018.05.189.
27. Garcia TA, Tamura Ozaki GA, Castoldi RC, Koike TE, Trindade Camargo RC, Silva Camargo Filho JC. Fractal dimension in the evaluation of different treatments of muscular injury in rats. Tissue Cell. 2018;54:120-126. doi: 10.1016/j.tice.2018.08.014.
28. Krause Neto W, de Assis Silva W, Polican Ciena A, et al. Total training load may explain similar strength gains and muscle hypertrophy seen in aged rats submitted to resistance training and anabolic steroids. Aging Male. 2018;21(1):65-76. doi: 10.1080/13685538.2017.1365832.
29. Tarawan VM, Gunadi JW, Setiawan, et al. Alteration of Autophagy Gene Expression by Different Intensity of Exercise in Gastrocnemius and Soleus Muscles of Wistar Rats. J Sports Sci Med. 2019;18(1):146-54.
30. Moreno-Cabañas A, Ortega JF, Morales-Palomo F, Ramirez-Jimenez M, Alvarez-Jimenez L, Mora-Rodriguez R. Concurrent endurance and resistance training enhances muscular adaptations in individuals with metabolic syndrome. Scand J Med Sci Sports. 2021;31(7):1440-9. doi: 10.1111/sms.13950.
31. de Sousa Neto IV, Carvalho MM, Marqueti RC, et al. Proteomic changes in skeletal muscle of aged rats in response to resistance training. Cell Biochem Funct. 2020;38(4):500-9. doi: 10.1002/cbf.3497.
32. Kordi M, Khoramshahi S, Eshghi S, Gaeeni A, Moosakhani A. The effect of high intensity interval training on some atrophic and anti-atrophic gene expression in rat skeletal muscle with diabetes. Sci Sports. 2020;35(3):e75-81. doi: 10.1016/j.scispo.2019.04.003.
33. Honda Y, Takahashi A, Tanaka N, et al. Muscle contractile exercise through a belt electrode device prevents myofiber atrophy, muscle contracture, and muscular pain in immobilized rat gastrocnemius muscle. PLoS One. 2022;17(9):e0275175. doi: 10.1371/journal.pone.0275175.
34. Kim JC, Kang YS, Noh EB, et al. Concurrent treatment with ursolic acid and low-intensity treadmill exercise improves muscle atrophy and related outcomes in rats. Korean J Physiol Pharmacol. 2018;22(4):427-36. doi: 10.4196/kjpp.2018.22.4.427.
35. Deval C, Calonne J, Coudy-Gandilhon C, et al. Mitophagy and Mitochondria Biogenesis Are Differentially Induced in Rat Skeletal Muscles during Immobilization and/or Remobilization. Int J Mol Sci. 2020;21(10):3691. doi: 10.3390/ijms21103691.
36. Slimani L, Micol D, Amat J, et al. The worsening of tibialis anterior muscle atrophy during recovery post-immobilization correlates with enhanced connective tissue area, proteolysis, and apoptosis. Am J Physiol Endocrinol Metab. 2012;303(11):E1335-47. doi: 10.1152/ajpendo.00379.2012.
37. Wang F, Zhou T, Zhou CX, Zhang QB, Wang H, Zhou Y. The worsening of skeletal muscle atrophy induced by immobilization at the early stage of remobilization correlates with BNIP3-dependent mitophagy. BMC Musculoskelet Disord. 2023;24(1):632. doi: 10.1186/s12891-023-06759-2.
38. da Mata GE, Bricola R, Ribeiro DN, et al. Acute exercise modulates Trim63 and Bmal1 in the skeletal muscle of IL-10 knockout mice. Cytokine. 2024;175:156484. doi: 10.1016/j.cyto.2023.156484.
39. Fávero PF, Vieira de Lima VA, Helena Dos Santos P, et al. Differential fractal dimension is associated with extracellular matrix remodeling in developing bovine corpus luteum. Biochem Biophys Res Commun. 2019;516(3):888-93. doi: 10.1016/j.bbrc.2019.06.002.
40. Lourenço Í, Krause Neto W, Amorim LDSP, et al. Previous short-term use of testosterone propionate enhances muscle hypertrophy in Wistar rats submitted to ladder-based resistance training. Tissue Cell. 2022;75:101741. doi: 10.1016/j.tice.2022.101741.
41. Von Walden F, Rea M, Mobley CB, et al. The myonuclear DNA methylome in response to an acute hypertrophic stimulus. Epigenetics. 2020;15(11):1151-62. doi: 10.1080/15592294.2020.1755581.
42. Hansson KA, Solbrå AV, Gundersen K, Bruusgaard JC. Computational Assessment of Transport Distances in Living Skeletal Muscle Fibers Studied In Situ. Biophys J. 2020;119(11):2166-78. doi: 10.1016/j.bpj.2020.10.016.
43. Murach KA, White SH, Wen Y, et al. Differential requirement for satellite cells during overload-induced muscle hypertrophy in growing versus mature mice. Skelet Muscle. 2017;7(1):14. doi: 10.1186/s13395-017-0132-z.
44. Gumpenberger M, Wessner B, Graf A, et al. Remodeling the Skeletal Muscle Extracellular Matrix in Older Age-Effects of Acute Exercise Stimuli on Gene Expression. Int J Mol Sci. 2020;21(19):7089. doi: 10.3390/ijms21197089.
45. Kritikaki E, Asterling R, Ward L, Padget K, Barreiro E, Simoes DCM. Exercise Training-Induced Extracellular Matrix Protein Adaptation in Locomotor Muscles: A Systematic Review. Cells. 2021;10(5):1022. doi: 10.3390/cells10051022.
46. Mayer WP, Baptista JDS, De Oliveira F, Mori M, Liberti EA. Consequences of ankle joint immobilisation: insights from a morphometric analysis about fibre typification, intramuscular connective tissue, and muscle spindle in rats. Histochem Cell Biol. 2021;156(6):583-94. doi: 10.1007/s00418-021-02027-3.
47. Lubin P, Zidi M. Mechanical properties change of immobilized skeletal muscle in short position measured by shear wave elastography and pure shearing test. J Mech Behav Biomed Mater. 2024;150:106317. doi: 10.1016/j.jmbbm.2023.106317.

48. Mavropalias G, Boppart M, Usher KM, Grounds MD, Nosaka K, Blazevich AJ. Exercise builds the scaffold of life: muscle extracellular matrix biomarker responses to physical activity, inactivity, and aging. Biol Rev Camb Philos Soc. 2023;98(2):481-519. doi: 10.1111/brv.12916.
49. Holwerda AM, Weijzen MEG, Zorenc A, et al. One Week of Single-Leg Immobilization Lowers Muscle Connective Protein Synthesis Rates in Healthy, Young Adults. Med Sci Sports Exerc. 2024;56(4):612-22. doi: 10.1249/MSS.0000000000003342.
50. Azizi E, Deslauriers AR, Holt NC, Eaton CE. Resistance to radial expansion limits muscle strain and work. Biomech Model Mechanobiol. 2017;16(5):1633-43. doi: 10.1007/s10237-017-0909-3.
51. Counts BR, Buckner SL, Mouser JG, et al. Muscle growth: To infinity and beyond? Muscle Nerve. 2017;56(6):1022-30. doi: 10.1002/mus.25696.
52. Ji LL, Yeo D. Mitochondrial dysregulation and muscle disuse atrophy. F1000Res. 2019;8:F1000 Faculty Rev-1621. doi: 10.12688/f1000research.19139.1.
53. Wu YF, Lapp S, Dvoretskiy S, et al. Optimization of a pericyte therapy to improve muscle recovery after limb immobilization. J Appl Physiol (1985). 2022;132(4):1020-30. doi: 10.1152/japplphysiol.00700.2021.
54. Kumar A, Raorane CJ, Rawat D, et al. Atenolol Ameliorates Skeletal Muscle Atrophy and Oxidative Stress Induced by Cast Immobilization in Rats. Biomedicines. 2023;11(5):1269. doi: 10.3390/biomedicines11051269.
55. Wyart E, Bindels LB, Mina E, Menga A, Stanga S, Porporato PE. Cachexia, a Systemic Disease beyond Muscle Atrophy. Int J Mol Sci. 2020;21(22):8592. doi: 10.3390/ijms21228592.
56. Roberts MD, Haun CT, Vann CG, Osburn SC, Young KC. Sarcoplasmic Hypertrophy in Skeletal Muscle: A Scientific "Unicorn" or Resistance Training Adaptation?. Front Physiol. 2020;11:816. doi: 10.3389/fphys.2020.00816.
57. Vann CG, Sexton CL, Osburn SC, et al. Effects of High-Volume Versus High-Load Resistance Training on Skeletal Muscle Growth and Molecular Adaptations. Front Physiol. 2022;13:857555. doi: 10.3389/fphys.2022.857555.
58. Haun CT, Vann CG, Osburn SC, et al. Muscle fiber hypertrophy in response to 6 weeks of high-volume resistance training in trained young men is largely attributed to sarcoplasmic hypertrophy. PLoS One. 2019;14(6):e0215267. doi: 10.1371/journal.pone.0215267.
59. Burd NA, West DW, Staples AW, et al. Low-load high volume resistance exercise stimulates muscle protein synthesis more than high-load low volume resistance exercise in young men. PLoS One. 2010;5(8):e12033. doi: 10.1371/journal.pone.0012033.